Chemical Science

ROYAL SOCIETY OF CHEMISTRY

EDGE ARTICLE

View Article Online
View Journal | View Issue

Cite this: *Chem. Sci.*, 2023, **14**, 10944

All publication charges for this article have been paid for by the Royal Society of Chemistry

Received 28th August 2023
Accepted 9th September 2023

DOI: 10.1039/d3sc04506d

rsc.li/chemical-science

Room temperature stable *E*,*Z*-diphosphenes: their isomerization, coordination, and cycloaddition chemistry†

Jieli Lin,[a] Shihua Liu,[a] Jie Zhang,[a] Hansjörg Grützmacher,[ab] Cheng-Yong Su[a] and Zhongshu Li*[a]

E,*Z*-isomers display distinct physical properties and chemical reactivities. However, investigations on heavy main group elements remain limited. In this work, we present the isolation and X-ray crystallographic characterization of N-heterocyclic vinyl (NHV) substituted diphosphenes as both *E*- and *Z*-isomers (L=CH–P=P–CH=L, *E*,*Z*-**2b**; L = N-heterocyclic carbene). *E*-**2b** is thermodynamically more stable and undergoes reversible photo-stimulated isomerization to *Z*-**2b**. The less stable *Z*-isomer *Z*-**2b** can be thermally reverted to *E*-**2b**. Theoretical studies support the view that this *E* ↔ *Z* isomerization proceeds *via* P=P bond rotation, reminiscent of the isomerization observed in alkenes. Furthermore, both *E*,*Z*-**2b** coordinate to an AuCl fragment affording the complex [AuCl(η^2-*Z*-**2b**)] with the diphosphene ligand in *Z*-conformation, exclusively. In contrast, *E*,*Z*-**2b** undergo [2 + 4] and [2 + 1] cycloadditions with dienes or diazo compounds, respectively, yielding identical cycloaddition products in which the phosphorus bound NHV groups are in *trans*-position to each other. DFT calculations provide insight into the *E*/*Z*-isomerisation and stereoselective formation of Au(I) complexes and cycloaddition products.

Introduction

Stable compounds containing a double bond between almost every p-block element have been reported since the independent landmark discoveries of a disilene, $Mes_2Si{=}SiMes_2$ (ref. 1), and a diphosphene, Mes*P=PMes*[2] (**A**, Fig. 1a), in 1981.[3] The species containing heavy main group elements often exhibit unique structures and reactivity patterns compared to their lighter congeners. Some are characterized by "*trans*-bent" E=E double bonds (that is, the molecule $R_2E{=}ER_2$ is not planar but shows ER_2 interplanar angles >0°) and show unique reactivity.[3a–e,g–i] The kinetic barriers for oligo/polymerization are much lower than for the lighter congeners with E = element from the second period, and the successful isolation of compounds with E from the higher periods requires the utilization of sterically encumbering substituents to introduce kinetic protection. Consequently, *cis*-folded isomers of $R_2E{=}ER_2$ or *Z*-isomers of RE=ER with heavy main group elements are rare due to increased steric repulsion caused by these substituents.[3a,b,d,4]

Diphosphenes are particularly intriguing; due to the diagonal relationship in the periodic table between carbon and phosphorus they behave to a certain extent like olefins.[3b,d,5] Numerous *E*-diphosphenes were fully characterized, but the synthesis and isolation of *Z*-diphosphenes remains challenging.[4e,6] The first spectroscopic detection of transient *Z*-diphosphene, *Z*-**A**, was found by laser irradiation of *E*-**A** at −80 °C. *Z*-**A** would revert back to the thermodynamically more stable *E*-**A** upon warming the solution to room temperature (RT) (Fig. 1a).[6b,c] Remarkably, Niecke *et al.* have isolated and crystallographically characterized a series of *Z*-diphosphenes (*Z*-RP=PMes*, R = ^{t}Bu(H)N, adamantyl(H)N, Et_3C(H)N, 2,4,6-^{i}PrC_6H_2(H)N, $(Me_3Si)_2N(SiMe_3)$N, **B**, Fig. 1b).[7] Among these, one diphosphene RP=PMes* with a sterically very demanding amido substituent [R = $(Me_3Si)_2N(SiMe_3)$N] could be isolated as both the *E*- and *Z*-isomers. These compounds displayed *E*,*Z*-isomerization in solution at RT.[7b] To the best of our knowledge, this is the only example where both the *E*- and *Z*-isomers of identical molecular composition could be isolated, although these amido-substituted diphosphenes undergo slow metatheses reactions at RT yielding symmetrical diphosphenes Mes*P=PMes* and RP=PR, likely *via* cyclotetraphosphanes formed in head-to-head dimerizations as intermediates (Fig. 1b). More recently, both diphosphasilene[6a] and diphosphene[8] substituted *Z*-diphosphene, [Si]=P–P=P–P=[Si] ([Si] = $[PhC(NtBu)_2SiN(SiMe_3)_2]$) and L=P–P=P–P=L (L = N-

[a]*LIFM, IGCME, School of Chemistry, Sun Yat-Sen University, Guangzhou 510006, China. E-mail: lizhsh6@mail.sysu.edu.cn*

[b]*Department of Chemistry and Applied Biosciences, ETH Zürich, Vladimir-Prelog-Weg 1, Zürich 8093, Switzerland*

† Electronic supplementary information (ESI) available: Synthesis and characterization of compounds, NMR spectra, and crystallographic and computational details. CCDC 2245822–2245824 and 2270969–2270971. For ESI and crystallographic data in CIF or other electronic format see DOI: https://doi.org/10.1039/d3sc04506d

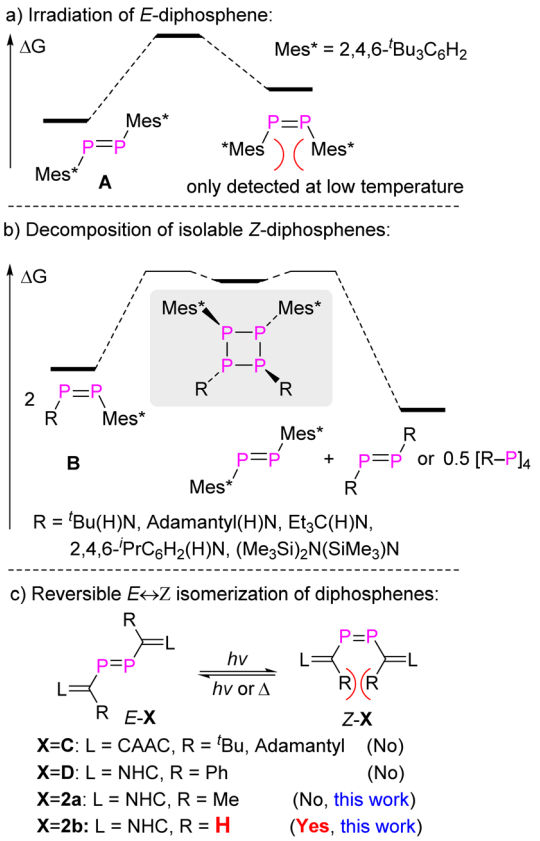

Fig. 1 Schematic representation of (a) irradiation of isolable *E*-diphosphene; (b) decomposition of isolable *Z*-diphosphenes; and (c) reversible *E* ↔ *Z* isomerization of isolable diphosphenes.

heterocyclic carbene (NHC)), were reported but likewise show limited stability.

Nevertheless, the presence of the RR′N–P=P or R=P–P=P–P=R fragments in *Z*-diphosphenes[6a,7] indicates some structural and electronic features for constructing stable *Z*-diphosphenes: (i) the sterically protecting group points away from the central P=P group to impose sufficient kinetic stability while at the same time the steric repulsion between the two substituents in *Z*-conformation is minimized. (ii) Electron delocalization as provided by co-planar moderately π-electron donating groups across the P=P bond should increase the thermodynamic stability of both the *E*- and *Z*-isomers. We therefore reasoned that N-heterocyclic vinyl (NHV = L=CR) substituted diphosphenes of the type L=CR–P=P–CR=L could likewise be promising candidates for the observation and eventual isolation of persistent *Z*-diphosphenes. Both the groups of Stephan and Ghadwal independently reported NHV-substituted *E*-diphosphenes L=C(R)–P=P–C(R)=L, ***E*-C** (L = cyclic alkyl amino carbene (CAAC), R = ^{t}Bu, adamantyl)[9] and ***E*-D** (L = NHC, R = phenyl)[10] (Fig. 1c). In these compounds, the presence of bulky R substituents on the NHV groups prevent the observation of the corresponding *Z*-isomers. In this study, we have successfully isolated and characterized diphosphene L=C(R)–P=P–C(R)=L **2b** in both *E*- and *Z*-configurations using the smallest possible substituent R = H. Specifically, ***E*-2b** can be converted reversibly to ***Z*-2b** by a photo-stimulated process while ***Z*-2b** is reverted to ***E*-2b** by a thermal process. Notably, only a slight increase in bulkiness in passing from R = H to Me allows only the *E*-isomer ***E*-2a** to be detected (Fig. 1c). The thermodynamic and kinetic parameters for *E*/*Z*-isomerisation as well as differences in coordination and cyclo-addition reactions between *E*- and *Z*-**2b** could be studied.

Results and discussion

Synthesis and characterization of 2a and 2b

NHV substituted dichlorophosphines **1a** (R = Me) and **1b** (R = H) (L=C(R)–PCl$_2$, L = SIPr = 1,3-bis-(2,6-diisopropylphenyl) imidazoline-2-ylidine) were prepared as white powders [**1a**: $\delta(^{31}P)$ = 191.9 ppm; **1b**: $\delta(^{31}P)$ = 183.7 ppm; see the ESI† for further details].[10,11] Treatment of **1a** with excess Mg powder in tetrahydrofuran (THF) at RT under vigorous stirring overnight in the dark afforded exclusively ***E*-2a** (L=C(Me)–P=P–C(Me)=L), which is photolytically and thermally stable. After work-up, ***E*-2a** was obtained in pure form as a red powder in 78% yield. Reaction of **1b** with Mg powder under the same conditions afforded a mixture of ***E*-2b** and ***Z*-2b** (L=C(H)–P=P–C(H)=L) in a ratio of 1.0 : 0.3 (Fig. 2a). After evaporation of THF, the solid residue was treated with toluene in order to extract the mixture of *E*/*Z*-**2b** from MgCl$_2$. Heating this solution of *E*/*Z*-**2b** at 110 °C for 20 minutes in the dark led to an enrichment of ***E*-2b** (***E*-2b** : ***Z*-2b** = 1.0 : 0.1). In contrast, irradiation of the toluene solution of

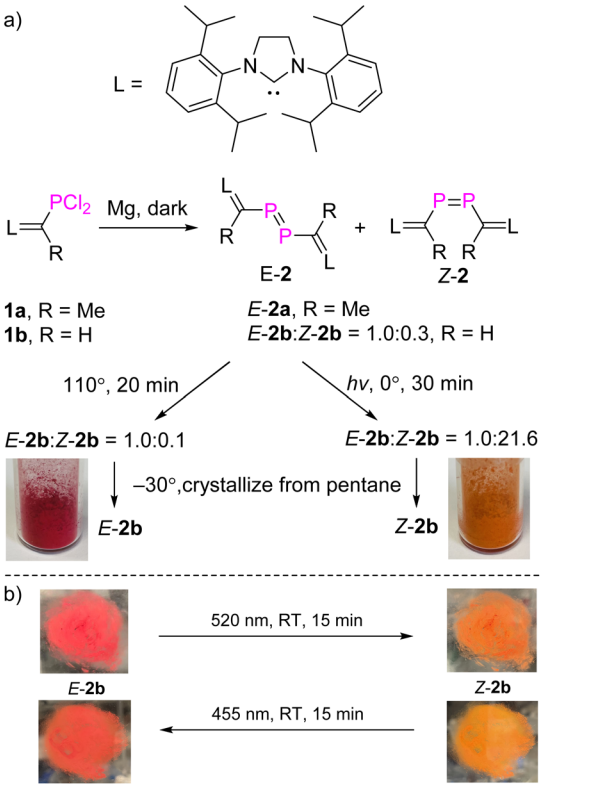

Fig. 2 (a) Synthesis of compounds **2a** and **2b**; (b) the *E* → *Z* isomerization of *E*-**2b** in the solid state as a thin layer in between two glass plates.

the mixture of *E*/*Z*-**2b** with UV light (Hg lamp) or LED light (520 nm) at 0 °C for 30 minutes led to the predominant formation of *Z*-**2b** (*E*-**2b** : *Z*-**2b** = 1.0 : 21.6). Evaporation of solvent toluene from these reaction mixtures after irradiation or heating, and recrystallization of the solid residues from cold pentane at −30 °C yielded a highly air-sensitive red crystalline powder of *E*-**2b** or a crystalline orange powder of *Z*-**2b** in 62% and 67% yields, respectively.

Multi-nuclear NMR spectra, single crystal X-ray diffraction (XRD), and high-resolution mass spectrometry were applied to characterize and confirm the molecular structures of *E*-**2a**, *E*-**2b**, and *Z*-**2b**. Characteristic singlet resonances at $\delta(^{31}P) = 382.6$, 379.6, or 259.5 ppm were observed in the ^{31}P NMR spectra of *E*-**2a**, *E*-**2b**, and *Z*-**2b**, respectively. These ^{31}P NMR shifts at high frequencies are within the range observed for other diphosphenes as well. In agreement with literature reported data, *E*-configured diphosphenes show resonances by about 100 ppm at higher frequencies compared to those of the *Z*-isomers.[6g,12] In the ^{1}H NMR spectra, singlet resonances at $\delta(^{1}H) = 1.85$ (*E*-**2a** PCCH_3), $\delta(^{1}H) = 4.98$ (*E*-**2b** PC*H*), and $\delta(^{1}H) = 4.61$ ppm (*Z*-**2b** PCH) are attributed to the protons of the R substituents at the NHV moieties, respectively.

The stereo-configurations of **2a** and **2b** are confirmed unambiguously by XRD methods (Fig. 3). The P=P bond lengths in the *E*-configured isomers *E*-**2a** [2.052(7) Å] and *E*-**2b** [2.0685(12) Å], and the one in the *Z*-isomer *Z*-**2b** [2.058(6) Å] are remarkably similar and typical of P=P double bonds [Σr_{cov}(P–P) = 2.22 Å, Σr_{cov}(P=P) = 2.04 Å].[13] The P–C and C=C bonds [1.765(3)–1.7863(13) Å and 1.362(4)–1.375(2) Å] vary only slightly in **2a** and **2b** and are typical of π-conjugated delocalized P=C or C=C bonds [Σr_{cov}(P–C) = 1.86 Å, Σr_{cov}(P=C) = 1.69 Å, Σr_{cov}(C–C) = 1.50 Å, Σr_{cov}(C=C) = 1.34 Å].[13a,b] As expected, the C–P=P–C fragments are nearly planar in *E*-**2a** (∠CPPC = 0.0°) and *E*-**2b** (∠CPPC = 0.2°), but show a small deviation from planarity in *Z*-**2b** (∠CPPC = 13.3°) indicating a higher steric congestion in the *Z*-isomer.

Toluene solutions of the *E*-configured isomers *E*-**2a** and *E*-**2b** are deep red and show strong absorptions at $\lambda_{max} = 518$ (1.8×10^4 M^{-1} cm^{-1}) and 534 nm (1.8×10^4 M^{-1} cm^{-1}). The *Z*-isomer *Z*-**2b** exhibits a strong absorption at lower wavenumbers with $\lambda_{max} = 482$ nm (2.3×10^4 M^{-1} cm^{-1}). In combination with TD-DFT calculations (Fig. S73–S78†), these absorptions are mainly attributed to the allowed π–π* transitions (HOMO → LUMO). The larger HOMO–LUMO gap of the *Z*-isomer is due to a lower HOMO energy (*Z*-**2b**: −5.27 eV *vs.* *E*-**2b**: −5.06 eV) and a higher LUMO energy (*Z*-**2b**: −0.44 eV *vs.* *E*-**2b**: −0.51 eV). In addition, all compounds show a very weak absorption at shorter wavelengths, namely 416 (2.5×10^3 M^{-1} cm^{-1}), 401 (3.0×10^3 M^{-1} cm^{-1}), and 359 (2.3×10^3 M^{-1} cm^{-1}) nm for *E*-**2a**, *E*-**2b**, and *Z*-**2b**, respectively (Fig. 4a). These are assigned to the forbidden n–π* transitions (HOMO−1 → LUMO). Comparable results have been reported for the structurally similar **D** (Fig. 1d).[10] Note, however, that in aryl substituted diphosphenes such as Mes*P=PMes* the ordering of these transitions is inverted and the n–π* is at higher wavenumbers while the π–π* occurs at shorter wavenumbers.[14]

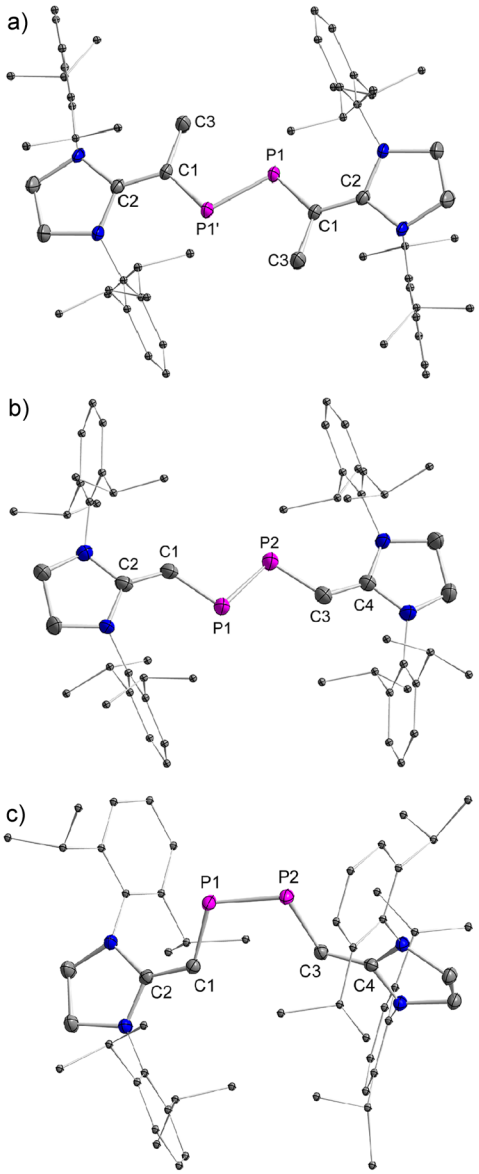

Fig. 3 Plots of the molecular structure of *E*-**2a**, *E*-**2b** and *Z*-**2b** (ellipsoids are set to 50% probability; H atoms and solvents are omitted for clarity). Selected distances (Å): (a) *E*-**2a**: P1–P1′ 2.0520(7), P1–C1 1.7863(13), C1–C2 1.3689(18), C1–C3 1.5127(19); (b) *E*-**2b**: P1–P2 2.0685(12), P1–C1 1.772(3), P2–C3 1.765(3), C1–C2 1.362(4), C3–C4 1.362(4); (c) *Z*-**2b**: P1–P2 2.0580(6), P1–C1 1.7848(16), P2–C3 1.7744(16), C1–C2 1.368(2), C3–C4 1.375(2).

E,*Z*-isomerization of *E*-2b and *Z*-2b

In the solid state and under an inert atmosphere, *E*,*Z*-**2b** are indefinitely stable even at elevated temperature in the dark. Upon irradiation, a gradually reversible *E*-**2b** ↔ *Z*-**2b** conversion is observed, which is indicated by a colour change of the microcrystalline powder from red to orange or *vice versa* (Fig. 2b). Similar observations were reported for alkenes or azo species.[15] In solution, *E*-**2b** is stable for days, whereas *Z*-**2b** slowly isomerizes to the thermodynamically more favourable *E*-**2b**. For example, approximately 10% of *Z*-**2b** converted to *E*-**2b** after two days as monitored by ^{31}P NMR spectra. Upon

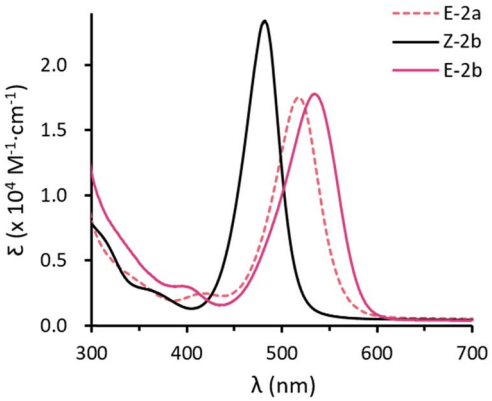

Fig. 4 UV-vis absorption spectra for toluene solution of *E*-**2a** (dashed red), *E*-**2b** (red) and *Z*-**2b** (black).

irradiation, *E*-**2b** isomerizes to *Z*-**2b** at 520 nm and reverts back to *E*-**2b** at 455 nm. No significant decomposition is observed for either *E*- or *Z*-**2b** upon irradiation or prolonged heating for hours. Some *E*-diphosphenes decompose upon irradiation,[6b,c,16] but may become stable upon irradiation when armed with extremely bulky substituents.[17] In contrast, all reported *Z*-diphosphenes show limited stability and decompose even at RT in solution.[6a–c,7,18] Therefore, *Z*-**2b** represents a very rare isolable *Z*-diphosphene with good thermal and photolytic stability at RT.[7,18]

The kinetics for the $E \leftrightarrow Z$ isomerization of **2b** was probed by ^{1}H NMR spectroscopy using hexamethylenetetramine as an internal standard. The pseudo-first-order rate constants (k) were calculated based on the consumption of the *E*-**2b** or *Z*-**2b** for photo- or thermally stimulated *E*,*Z*-isomerization. The plots of ln[*E*-**2b**] *vs.* *t* (Fig. 5a) and ln[*Z*-**2b**] *vs.* *t* (Fig. S59† and 5b) indicate first order kinetics with $k_{520\text{nm}} = 4.4 \times 10^{-3}$ s^{-1}, $k_{455\text{nm}} = 1.0 \times 10^{-2}$ s^{-1}, and $k_{348.15\text{K}} = 5.6 \times 10^{-4}$ s^{-1}, respectively. The photostationary (PSS) equilibria were established within 300 s or 750 s for the *E*-**2b** → *Z*-**2b** or *E*-**2b** ← *Z*-**2b** isomerization process yielding a mixture of *E*-**2b** : *Z*-**2b** = 0.19 or 4.40 under irradiation at 520 or 455 nm, respectively. The relative molar extinction coefficient of *E*,*Z*-**2b** at 520 or 455 nm was determined to be *Z*-**2b** : *E*-**2b** = 0.18 or 4.76 (see Fig. S50 and S51† for details). These results fit well to eqn (1) for the PSS ensuring equal quantum yields (Φ) for the photoisomerization reactions in both directions.[19]

$$\left(\frac{E}{Z}\right)_{\text{PSS}} = \frac{(\varepsilon_Z)}{(\varepsilon_E)} \times \frac{(\Phi_{Z\rightarrow E})}{(\Phi_{E\rightarrow Z})} \quad (1)$$

Furthermore, the temperature dependence of the isomerization rate constructed from the kinetic data measured at 5 K intervals from 348.15 K to 368.15 K gives the experimental activation energy for the thermal *Z*-**2b** → *E*-**2b** conversion as $E_a = 23.4 \pm 0.9$ kcal mol^{-1}. The pre-exponential factor can be expressed at these temperatures by the Arrhenius equation $k = 2.72 \times 10^{11} \times e^{-23.4/RT}$ (Fig. 5c). This high pre-exponential factor precludes the population of excited triplet states in the thermal *Z*-**2b** → *E*-**2b** isomerization process.[20] The Eyring plot

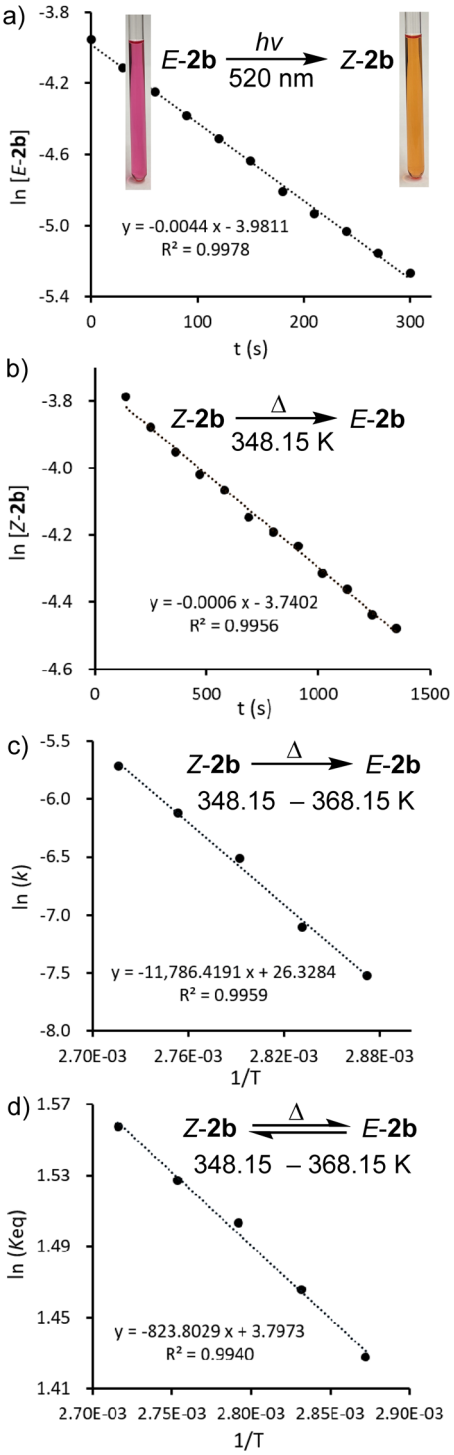

Fig. 5 Plots of (a) ln[*E*-**2b**] against reaction time *t* under irradiation at 520 nm; (b) ln[*E*-**2a**] against reaction time *t* at 348.15 K; (c) ln(k) against 1/*T*; and (d) ln(K_{eq}) against 1/*T* at 348.15 K to 368.15 K.

constructed from these data affords the experimental activation parameters as $\Delta H^{\ddagger} = 22.7 \pm 0.9$ kcal mol^{-1}, $\Delta S^{\ddagger} = -8.6 \pm 2.4$ e.u., and $\Delta G^{\ddagger}_{(298.15\text{K})} = 25.3 \pm 1.6$ kcal mol^{-1} (Fig. S64†). The activation barrier of the thermal isomerization is comparable to those of the previously reported diphosphenes Mes*P═PMes* [$\Delta G^{\ddagger}_{(273\text{K})} = 20.3$ kcal mol^{-1}][6b] and RP═PMes* ($\Delta G^{\ddagger}_{(293\text{K})} =$

25.5 kcal mol^{-1}, R = $(Me_3Si)_2N(Me_3Si)N$, Fig. 1b).[7b] For comparison, the activation barriers for stilbene[21] or azobenzene[22] are about 40 or 23 kcal mol^{-1}, respectively. Moreover, a van't Hoff analysis ($\Delta H = 1.6 \pm 0.1$ kcal mol^{-1}, $\Delta S = 7.6 \pm 0.2$ e.u.) revealed that the free energy of *Z*-**2b** is slightly lower, $\Delta G_{(298.15K)} = -0.6 \pm 0.1$ kcal mol^{-1}, than that of *E*-**2b** (Fig. 5d). In conclusion, these special factors (small energy difference between *E*- and *Z*-**2b** and relatively high activation barrier for the thermal *Z*-**2b** → *E*-**2b** isomerization process) allow the isolation of diphosphene **2b** in both *E*- and *Z*-configurations.

To provide a deeper understanding of the *E*,*Z*-isomerization mechanism, density functional theory (DFT) calculations were carried out at the M062X-D3/Def2TZVP-SMD(toluene)//M062X-D3/Def2SVP level of theory.[23] Apart from *E*,*Z*-**2b** we included also the methyl-substituted derivates *E*,*Z*-**2a** in this study although an *E*/*Z*-isomerism could not be observed experimentally. Possible minimum energy reaction pathways (MERPs) for both the photolytic *E*-**X** ↔ *Z*-**X** and thermal *Z*-**X** → *E*-**X** (X = **2a**, **2b**) are shown in Fig. 6. Upon irradiation, *E*-**2a** and *E*-**2b** are excited to the triplet states ^{3}T-**2a** (26.7 kcal mol^{-1}) and ^{3}T-**2b** (23.6 kcal mol^{-1}).[24] The structures of the triplet states ^{3}T-**2a** and ^{3}T-**2b** are very similar and notably contain a significantly elongated P–P bond (2.21 Å), which is in the range of a single bond, and C–P–P–C dihedral angles of 106.0°. These structures are very different compared to the singlet ground state structures of *E*-**2a** and *E*-**2b** (P=P: 2.05 Å; C–P–P–C = 180.0°). Subsequently, these excited triplet states relax *via* a spin flipping process to the *E*- or *Z*-isomers in their singlet ground states in exergonic reactions. In case of **2a**, the resulting *Z*-**2a** will quickly isomerize to the thermodynamically more stable *E*-**2a** (−11.2 kcal mol^{-1}) *via* a relatively small activation barrier TS**R**-**2a** (13.9 kcal mol^{-1}). In case of **2b**, the *E*/*Z* ratio of the resulting mixture depends on the relative molar extinction coefficient of *E*,*Z*-**2b**. At elevated temperatures, *Z*-**2b** isomerizes *via* the activated complexes TS**R**-**2b** (22.7 kcal mol^{-1}), which has a singlet electronic configuration, affording the thermodynamically more stable *E*-isomers *E*-**b** (−3.3 kcal mol^{-1}). The calculations are in good agreement with the experimental observations: *Z*-**2a** cannot be detected because of its thermodynamic instability *versus* *E*-**2a** (+11.2 kcal mol^{-1}) and low activation barrier for the thermal isomerization (E_a = 13.9 kcal mol^{-1}). On the other hand, *Z*-**2b** can be isolated because it is almost isoenergetic with *E*-**2b** and E_a for the thermal isomerization is much higher (25.3 ± 1.6 kcal mol^{-1}). Note that the calculated activation barriers predicted at the same level of theory for the *Z* → *E* isomerization process of the olefin stilbene [TS_R = 43.6 kcal mol^{-1} *vs.* 40 kcal mol^{-1} (exp.)][21] is much higher while the one of azobenzene [TS_I = 25.5 kcal mol^{-1} *vs.* 23 kcal mol^{-1} (exp.)][22] is in the same range (Fig. S79†). For comparison we also investigated possible *E*/*Z*-isomerization pathways for the simple divinyl substituted compound CH_2=CH–P=P–CH=CH_2 and found that the activation barrier E_a^R = 24.3 kcal mol^{-1} for a rotation around the P,P-bond is comparable to the one in *E*-**2b** (the activation barrier for inversion at one phosphorus center – an alternative process for *E*/*Z*-isomerization – is much higher in energy at E_a^I = 50.1 kcal mol^{-1}) (Fig. S80†). Similar data have been theoretically predicted for the *Z* → *E* isomerization of HP=PH (Fig. S81†).[25]

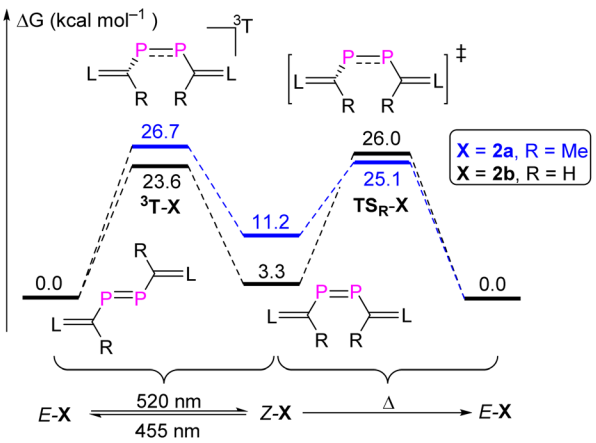

Fig. 6 MERP for the reversible photo- and thermally stimulated *E*,*Z*-isomerization of **2a** and **2b**.

Coordination chemistry of *E*-2b and *Z*-2b

Having the rare opportunity to have stable and pure *E*- and *Z*-isomers of a diphosphene of identical molecular composition at hand, we investigated the coordination chemistry *versus* an AuCl fragment and the cycloaddition chemistry *versus* dimethylbutadiene (DMBD) and (trimethylsilyl)diazomethane (TDM). Both reactivities are typical of olefins as hydrocarbon counterparts to diphosphenes. Remarkably, treatment of both *E*-**2b** and *Z*-**2b** with equimolar amounts of [AuCl(SMe$_2$)] in THF

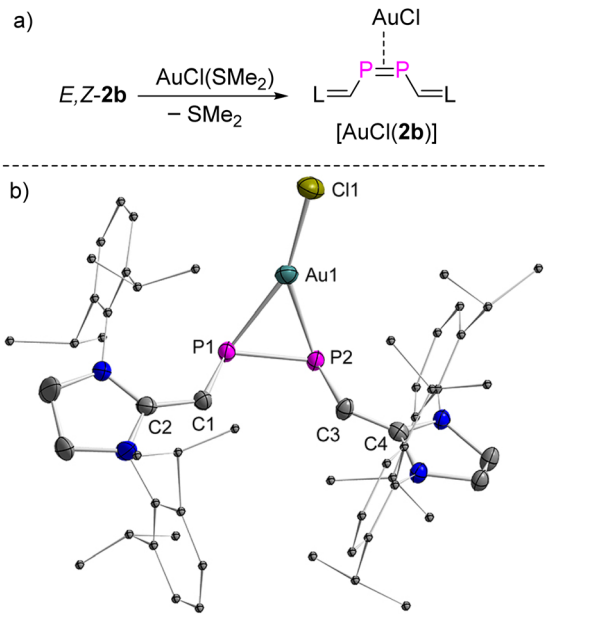

Fig. 7 (a) Synthesis of [AuCl(**2b**)]; (b) plot of the molecular structure of [AuCl(**2b**)] (thermal ellipsoids are set to 50% probability; H atoms and solvent molecules are omitted for clarity). Selected distances (Å): P1–P2 2.1254(14), P1–C1 1.754(4), P1–Au1 2.4580(11), P2–C3 1.753(4), P2–Au1 2.4280(11), Au1–Cl1 2.3357(12), C1–C2 1.389(6), C3–C4 1.377(5).

at RT afforded selectively the same complex within minutes. After work-up, compound [AuCl(**2b**)] was obtained as a deep red powder in 92% yield (Fig. 7a). A characteristic singlet resonance at $\delta(^{31}P) = 153.8$ ppm in the ^{31}P NMR spectrum indicates the formation of a symmetric complex. With respect to both *E*-**2b** [$\delta(^{31}P) = 379.6$ ppm] and *Z*-**2b** [$\delta(^{31}P) = 259.5$ ppm], a significant coordination shift $\Delta\delta = \delta_{complex} - \delta_{ligand}$ of −225.8 ppm or −105.7 ppm respectively, to lower frequencies, is observed.

The molecular structure of [AuCl(**2b**)] was determined by XRD methods (Fig. 7b) and shows that **2b** is (i) η^2-bound to the AuCl moiety and (ii) the substituents adopt a *cis*-configuration with respect to the P–P vector indicating that, remarkably and unexpectedly, the reaction of *E*-**2b** with [AuCl(SMe$_2$)] induces *E*-**2b** → *Z*-**2b** isomerization. In the complex [AuCl(η^2-*Z*-**2b**)], the P1–P2 bond length is elongated to 2.1254(12) Å with respect to uncoordinated *Z*-**2b** [2.0580(6) Å]. This observation indicates significant electron donation from the d^{10}-valence electron configured Au(I) ion into the π*(P=P) anti-bonding orbital. The Au–P1 and Au–P2 bonds are almost identical in length [P1–Au1: 2.4580(11) Å; P2–Au1: 2.4280(11) Å]. The metal center resides in a trigonal planar geometry [sum of bond angles Σ°(Au) = 359.8°]. The dihedral angle between the Au–P1–P2 and C1–P1–P2–C3 planes is 73.9°. Hand in hand with the elongation of the coordinated P=P bond goes a reduction of the ∠CPPC torsion angle from 13.3° (*Z*-**2b**) to 5.7° in the complex [AuCl(η^2-*Z*-**2b**)] indicating reduced steric repulsion between two NHV groups. To the best of our knowledge, [AuCl(η^2-*Z*-**2b**)] represents the first crystallographically characterized mononuclear η^2-*Z*-diphosphene complex and the only η^2-bound diphosphene Au(I) complex isolated so far (*vide infra*).[7,18,26]

DFT calculations were carried out in order to gain deeper insight into the selective formation of [AuCl(η^2-*Z*-**2b**)]. Both the full model and a simplified model complex [AuCl(η^2-*Z*-**2b^H**)] where the 2,6-diisopropylphenyl (Dipp) groups were replaced with H atoms were investigated at the BP86-D3BJ/Def2TZVP-SMD(THF)//BP86-D3BJ/Def2SVP level of theory (Fig. 8).[23] For the full model, the stability of four different conformers follows the order [AuCl(η^2-*Z*-**2b**)] (−1.8 kcal mol^{-1}) > [AuCl(η^1-*E*-**2b**)] (0 kcal mol^{-1}) > [AuCl(η^2-*E*-**2b**)] (0.1 kcal mol^{-1}) > [AuCl(η^1-*Z*-**2b**)] (4.4 kcal mol^{-1}). The highest activation barrier of 22.3 kcal mol^{-1} (**TS2-2b**) is attributed to the rotation of the P=P bond during the [AuCl(η^1-*E*-**2b**)] → [AuCl(η^1-*Z*-**2b**)] isomerization process, which is only slightly smaller than the calculated barrier for the *E*/*Z*-isomerization of the uncoordinated diphosphene. On the other hand, the conversion from η^1- to η^2-gold complexes for both *E*- and *Z*-isomers proceeds smoothly *via* **TS1-2b** (7.4 kcal mol^{-1}) and **TS3-2b** (0.6 kcal mol^{-1}). For the simplified model, similar energy barriers are obtained for the intramolecular conversion among these four conformers. However, the stability order differs and follows the order [AuCl(η^1-*E*-**2b^H**)] (0 kcal mol^{-1}) > [AuCl(η^1-*Z*-**2b^H**)] (0.3 kcal mol^{-1}) > [AuCl(η^2-*Z*-**2b^H**)] (0.6 kcal mol^{-1}) > [AuCl(η^2-*E*-**2b^H**)] (2.0 kcal mol^{-1}). The higher stability (although marginal) of the η^1-bound complexes agrees with the one previously reported for three Au(I) bisarene-substituted *E*-diphosphene complexes, in which the P=P bond is shortened with respect to the uncoordinated diphosphene.[26] Note that diphosphenes in *E*-configuration are frequently bound in η^2-fashion to other transition metal centers.[27]

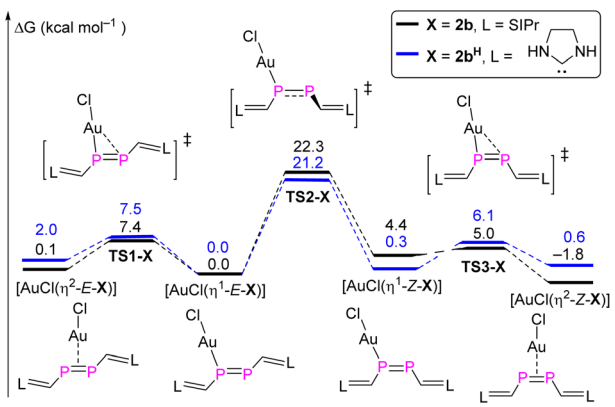

Fig. 8 MERP for the intramolecular conversion between η^1- and η^2-gold complexes with both models **2b** and **2b^H**.

Cycloaddition chemistry of *E*-2b and *Z*-2b

Treatment of *E*-**2b** with equimolar amounts of DMBD or TDM in toluene at RT resulted in rapid and quantitative conversion to yield the [2 + 4] and [2 + 1] cycloaddition products **3** and **4** within minutes (Fig. 9).[6g] The ^{31}P NMR spectra of **3** and **4** displayed a singlet at −68.0 ppm, a doublet of a doublet at −161.3 ppm ($^1J_{PP} = 158.3$ Hz, $^2J_{PH} = 29.36$ Hz) and a doublet at −181.9 ppm ($^1J_{PP} = 158.3$ Hz), respectively. Detailed characterization of three-membered heterocyclic diphosphiranes by multi-nuclear NMR spectroscopic methods has been reported by Jutzi and co-workers.[28] Notably, treatment of *Z*-**2b** with DMBD or TDM at RT afforded the same products **3** or **4**, respectively. However, complete conversion to **3** required more than 8 days or 6 hours to give **4** (Fig. S58 and S63†). The *E*-isomer *E*-**2b** was not detected in the course of these reactions. These findings suggest that *Z*-**2b** does not directly react with these substrates but first isomerizes to *E*-**2b**, which subsequently is rapidly consumed in the [2 + 4] or [2 + 1] cycloaddition. XRD studies unveiled the molecular structures of **3** and **4** and showed that in both cases the two N-heterocyclic vinyl groups are placed in mutual *trans*-position to each other (Fig. 10).

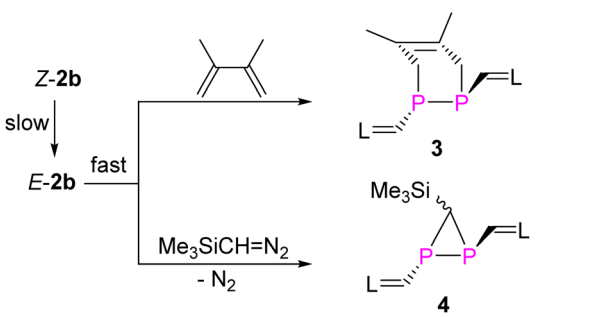

Fig. 9 Synthesis of **3** and **4**.

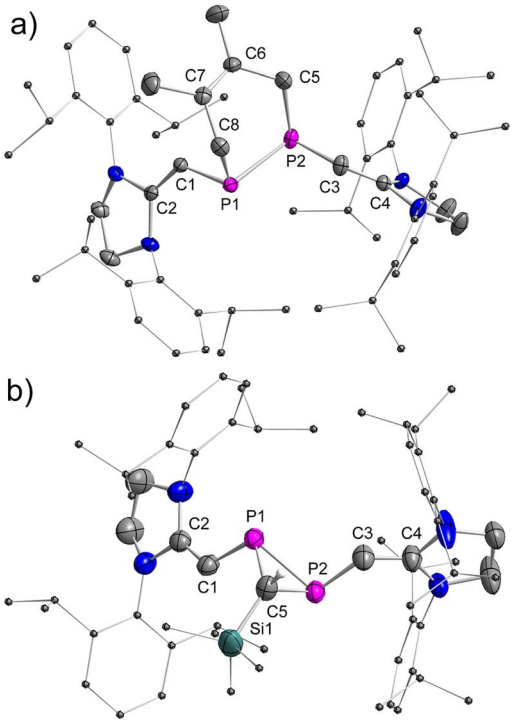

Fig. 10 Plot of the molecular structure of **3** and **4** (ellipsoids are set to 50% probability; H atoms except the one on C5 in **4** and solvents are omitted for clarity). Selected distances (Å): (a) **3**: P1–P2 2.2389(6), P1–C1 1.8202(16), C1–C2 1.369(2), P2–C3 1.8187(17), C3–C4 1.359(2), P1–C8 1.8999(17), C8–C7 1.512(2), C7–C6 1.352(3), C6–C5 1.505(2), C5–P2 1.9054(19); (b) **4**: P1–P2 2.2166(13), P1–C1 1.792(4), C1–C2 1.347(5), P2–C3 1.794(4), C3–C4 1.348(5), P1–C5 1.854(4), P2–C5 1.863(4), C5–Si1 1.854(4).

Again, DFT calculations were performed to provide a better understanding of the reactivity difference in between *E*-**2b** and *Z*-**2b**. The reaction mechanism for the [2 + 4] cycloaddition reaction between DMBD and model **2b** or $\mathbf{2b^H}$ was studied at the M062X-D3/Def2TZVP-SMD(toluene)//M062X-D3/Def2SVP level of theory (Fig. 11).[23] In both cases, the [2 + 4] cycloaddition reactions proceed in a concerted fashion *via* one activated complex at the corresponding transition states. In the reaction

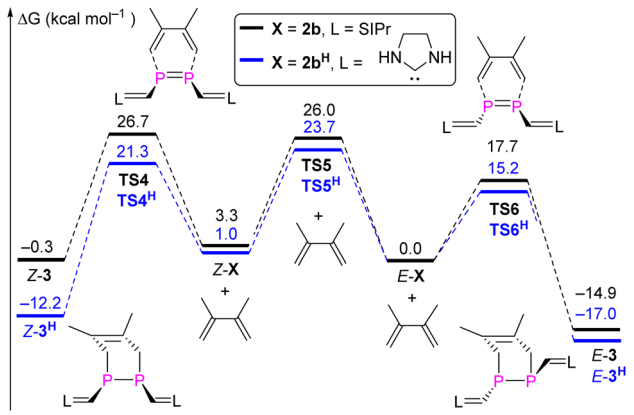

Fig. 11 MERP for the formation of **3** and $\mathbf{3^H}$.

between DMBD and the simplified *E*-configured model *E*-$\mathbf{2b^H}$ the transition state $\mathbf{TS6^H}$ (15.2 kcal mol^{-1}) is about 5 kcal mol^{-1} lower than the one for the reaction with *Z*-$\mathbf{2b^H}$ ($\mathbf{TS4^H}$ = 20.3 kcal mol^{-1} with respect to *Z*-$\mathbf{2b^H}$). Both products *E*-$\mathbf{3^H}$ (−17.0 kcal mol^{-1}) and *Z*-$\mathbf{5^H}$ (−12.2 kcal mol^{-1}) are formed in exergonic reactions, which differ by 4.8 kcal mol^{-1} in favour of the *E*-isomer. The kinetic and thermodynamic formation of the *E*-configured isomer becomes even more favourable in the reactions with the sterically more hindered *E*/*Z*-**2b** as diene acceptors. Here **TS6** on the MERP in the reaction with *E*-**2b** is lower by 9.0 kcal mol^{-1} than **TS4** (on the MERP with *Z*-**2b**) and the *E*-configured product *E*-**3** is more stable by 14.6 kcal mol^{-1} when compared to *Z*-**3**. The latter is formed in an almost thermoneutral reaction ($\Delta G_r = -3.6$ kcal mol^{-1}) between *Z*-**2b** and DMBD while the formation of the *E*-isomer *E*-**3** is exergonic by −14.9 kcal mol^{-1}. Not unexpected, with increasing steric encumbrance the transition state energies increase while the product stabilities decrease. But the calculated barriers for the [2 + 4] cycloaddition between *E*/*Z*-**2b** and DMBD are still relatively low and comparable to the barrier for *E* → *Z* isomerization to allow a reaction at room temperature, which ultimately leads selectively to the thermodynamically more stable product *E*-**3**. Thus, the calculations agree well with the experimental observations.

Conclusions

In contrast to the *E*/*Z* isomerization of olefins or azo compounds, for which this process was discovered more than eight decades ago in 1934 (ref. 21*a*) and 1937,[29] respectively, the direct observation of *E*,*Z*-isomerization for compounds with a double bond between two heavy main group elements remains scarce. Specifically, kinetic and thermodynamic data for these isomerizations are lacking as well as comprehensive investigations of their distinct physical properties and chemical reactivities. In this study, we present the successful isolation and unambiguous characterization of the *E*- and *Z*-isomers of a diphosphene (*E*,*Z*-**2b**). XRD studies show that both have a short P=P double bond of about the same length and confirm their stereo configuration. Kinetic studies reveal the first-order process for both photo- and thermally stimulated *E* ↔ *Z* isomerization. In combination, the experimental and theoretical data show that the *E* ↔ *Z* isomerization of diphosphene proceeds *via* rotation around the P=P double bond. However, a similar *E* ↔ *Z* isomerization has not been reported for the nitrogen analogue of *E*-**2b**.[30] Both *E*,*Z*-**2b** react with the AuCl fragment to afford exclusively the thermodynamically slightly more favoured complex [AuCl(η^2-*Z*-**2b**)], which is the first mononuclear metal complex of a diphosphene in *Z*-conformation. The activation barrier for *E* → *Z*-isomerisation of the η^1-bound AuCl complexes, which are intermediates on the MERP that give [AuCl(η^2-*Z*-**2b**)], is slightly smaller (≈4 kcal mol^{-1}) than in the uncoordinated diphosphene. It is presently not clear why in this particular case the Au(I) complex with *Z*-**2b** is more stable. The opposite is observed when a mixture of *E*/*Z*-**2b** is employed in a cycloaddition with a diene or diazo compound. Here, the *Z*-isomer is unreactive and must isomerize slowly to *E*-

2b in order to allow a reaction. Compound *E*-**2b** readily engages in a [2 + 4] or [2 + 1] cycloaddition reaction and as a consequence, exclusively the cycloaddition product with an *E*-arrangement of the substituents with respect to the P–P vector is obtained.

Data availability

The data generated in this study are available in the main text or the ESI.† Crystallographic data has been deposited at the joint Cambridge Crystallographic Data Centre (CCDC 2245822–2245824, 2270969–2270971). Synthesis and characterization of compounds, NMR spectra, crystallographic, and computational details are provided in the ESI.†

Author contributions

J. Lin carried out most of the experimental work. S. Liu and J. Zhang assisted with the NMR spectra and X-ray single crystallographic diffraction measurements. Z. Li carried out the computational studies. The manuscript was written through contributions of all authors. All authors have given approval to the final version of the manuscript.

Conflicts of interest

There are no conflicts to declare.

Acknowledgements

This work was supported by the National Natural Science Foundation of China (22271315, 22171291, 21821003, 21890380), Tip-top Scientific and Technical Innovative Youth Talents of Guangdong Special Support Program (2019TQ05C926), Guangdong Basic and Applied Basic Research Foundation (2021A1515012028, 2023A1515010092), Science and Technology Planning Project of Guangzhou (202102080189), National Key Research and Development Program of China (2021YFA1500401).

Notes and references

1 R. West, M. J. Fink and J. Michl, *Science*, 1981, **214**, 1343–1344.

2 M. Yoshifuji, I. Shima, N. Inamoto, K. Hirotsu and T. Higuchi, *J. Am. Chem. Soc.*, 1981, **103**, 4587–4589.

3 (*a*) M. Kira, *Proc. Jpn. Acad., Ser. B*, 2012, **88**, 167–191; (*b*) R. C. Fischer and P. P. Power, *Chem. Rev.*, 2010, **110**, 3877–3923; (*c*) Y. Wang and G. H. Robinson, *Chem. Commun.*, 2009, 5201–5213; (*d*) P. P. Power, *Chem. Rev.*, 1999, **99**, 3463–3504; (*e*) P. P. Power, *J. Chem. Soc., Dalton Trans.*, 1998, 2939–2951; (*f*) M. Fischer, M. M. D. Roy, L. L. Wales, M. A. Ellwanger, A. Heilmann and S. Aldridge, *J. Am. Chem. Soc.*, 2022, **144**, 8908–8913; (*g*) C. Weetman, *Chem.–Eur. J.*, 2021, **27**, 1941–1954; (*h*) V. Nesterov, N. C. Breit and S. Inoue, *Chem.–Eur. J.*, 2017, **23**, 12014–12039; (*i*) A. Rammo and D. Scheschkewitz, *Chem.–Eur. J.*, 2018, **24**, 6866–6885; (*j*) J. Li, Z. Lu and L. L. Liu, *J. Am. Chem. Soc.*, 2022, **144**, 23691–23697; (*k*) E. A. LaPierre, B. O. Patrick and I. Manners, *J. Am. Chem. Soc.*, 2023, **145**, 7107–7112.

4 (*a*) R. Holzner, A. Porzelt, U. S. Karaca, F. Kiefer, P. Frisch, D. Wendel, M. C. Holthausen and S. Inoue, *Dalton Trans.*, 2021, **50**, 8785–8793; (*b*) M. Kobayashi, N. Hayakawa, T. Matsuo, B. Li, T. Fukunaga, D. Hashizume, H. Fueno, K. Tanaka and K. Tamao, *J. Am. Chem. Soc.*, 2016, **138**, 758–761; (*c*) D. Wendel, T. Szilvási, C. Jandl, S. Inoue and B. Rieger, *J. Am. Chem. Soc.*, 2017, **139**, 9156–9159; (*d*) V. Y. Lee and A. Sekiguchi, *Organometallic Compounds of Low-Coordinate Si, Ge, Sn and Pb: From Phantom Species to Stable Compounds*, Wiley, 2011; (*e*) T. Sasamori and N. Tokitoh, *Dalton Trans.*, 2008, 1395–1408; (*f*) N. C. Breit, T. Szilvási and S. Inoue, *Chem. Commun.*, 2015, **51**, 11272–11275; (*g*) L. Zborovsky, A. Kostenko, D. Bravo-Zhivotovskii and Y. Apeloig, *Angew. Chem., Int. Ed.*, 2019, **58**, 14524–14528.

5 (*a*) K. B. Dillon, F. Mathey and J. F. Nixon, *Phosphorus: The Carbon Copy: From Organophosphorus to Phospha-organic Chemistry*, Wiley, 1998; (*b*) G. Rayner-Canham, *Found. Chem.*, 2011, **13**, 121–129; (*c*) F. Mathey, *Angew. Chem., Int. Ed.*, 2003, **42**, 1578–1604; (*d*) S. Wang, J. D. Sears, C. E. Moore, A. L. Rheingold, M. L. Neidig and J. S. Figueroa, *Science*, 2022, **375**, 1393–1397; (*e*) K. B. Dillon, V. C. Gibson and L. J. Sequeira, *J. Chem. Soc., Chem. Commun.*, 1995, 2429–2430; (*f*) R. C. Smith, E. Urnezius, K.-C. Lam, A. L. Rheingold and J. D. Protasiewicz, *Inorg. Chem.*, 2002, **41**, 5296–5299.

6 (*a*) S. Khan, R. Michel, S. S. Sen, H. W. Roesky and D. Stalke, *Angew. Chem., Int. Ed.*, 2011, **50**, 11786–11789; (*b*) A.-M. Caminade, M. Verrier, C. Ades, N. Paillous and M. Koenig, *J. Chem. Soc., Chem. Commun.*, 1984, 875–877; (*c*) Y. Masaaki, S. Takahiro and I. Naoki, *Chem. Lett.*, 1988, **17**, 1735–1738; (*d*) L. Weber, F. Ebeler and R. S. Ghadwal, *Coord. Chem. Rev.*, 2022, **461**, 214499; (*e*) N. Tokitoh, *J. Organomet. Chem.*, 2000, **611**, 217–227; (*f*) M. Yoshifuji, *J. Chem. Soc., Dalton Trans.*, 1998, 3343–3350; (*g*) L. Weber, *Chem. Rev.*, 1992, **92**, 1839–1906; (*h*) R. S. Ghadwal, *Acc. Chem. Res.*, 2022, **55**, 457–470.

7 (*a*) E. Niecke, B. Kramer and M. Nieger, *Angew. Chem., Int. Ed.*, 1989, **28**, 215–217; (*b*) E. Niecke, O. Altmeyer and M. Nieger, *Angew. Chem., Int. Ed.*, 1991, **30**, 1136–1138.

8 J. D. Masuda, W. W. Schoeller, B. Donnadieu and G. Bertrand, *J. Am. Chem. Soc.*, 2007, **129**, 14180–14181.

9 L. L. Liu, L. L. Cao, J. Zhou and D. W. Stephan, *Angew. Chem., Int. Ed.*, 2019, **58**, 273–277.

10 D. Rottschäfer, M. K. Sharma, B. Neumann, H.-G. Stammler, D. M. Andrada and R. S. Ghadwal, *Chem.–Eur. J.*, 2019, **25**, 8127–8134.

11 (*a*) I. C. Watson, A. Schumann, H. Yu, E. C. Davy, R. McDonald, M. J. Ferguson, C. Hering-Junghans and E. Rivard, *Chem.–Eur. J.*, 2019, **25**, 9678–9690; (*b*) C. Hering-Junghans, P. Andreiuk, M. J. Ferguson, R. McDonald and E. Rivard, *Angew. Chem., Int. Ed.*, 2017, **56**, 6272–6275.

12 M. Yoshifuji, *Eur. J. Inorg. Chem.*, 2016, **2016**, 607–615.

13 (*a*) P. Pyykkö and M. Atsumi, *Chem.–Eur. J.*, 2009, **15**, 12770–12779; (*b*) F. H. Allen, O. Kennard, D. G. Watson, L. Brammer, A. G. Orpen and R. Taylor, *J. Chem. Soc., Perkin Trans. 2*, 1987, S1–S19; (*c*) J. D. Protasiewicz, M. P. Washington, V. B. Gudimetla, J. L. Payton and M. Cather Simpson, *Inorg. Chim. Acta*, 2010, **364**, 39–45.

14 (*a*) A. H. Cowley, A. Decken, N. C. Norman, C. Krüger, F. Lutz, H. Jacobsen and T. Ziegler, *J. Am. Chem. Soc.*, 1997, **119**, 3389–3390; (*b*) H.-L. Peng, J. L. Payton, J. D. Protasiewicz and M. C. Simpson, *J. Phys. Chem. A*, 2009, **113**, 7054–7063.

15 (*a*) P. Naumov, S. Chizhik, M. K. Panda, N. K. Nath and E. Boldyreva, *Chem. Rev.*, 2015, **115**, 12440–12490; (*b*) M. Irie, T. Fukaminato, K. Matsuda and S. Kobatake, *Chem. Rev.*, 2014, **114**, 12174–12277; (*c*) H. Koshima, N. Ojima and H. Uchimoto, *J. Am. Chem. Soc.*, 2009, **131**, 6890–6891; (*d*) A. K. Bartholomew, I. B. Stone, M. L. Steigerwald, T. H. Lambert and X. Roy, *J. Am. Chem. Soc.*, 2022, **144**, 16773–16777.

16 (*a*) M. Yoshifuji, N. Shinohara and K. Toyota, *Tetrahedron Lett.*, 1996, **37**, 7815–7818; (*b*) Y. Masaaki, S. Takahiro and I. Naoki, *Bull. Chem. Soc. Jpn.*, 1989, **62**, 2394–2395; (*c*) V. Cappello, J. Baumgartner, A. Dransfeld, M. Flock and K. Hassler, *Eur. J. Inorg. Chem.*, 2006, **2006**, 2393–2405.

17 (*a*) S. Shah, M. C. Simpson, R. C. Smith and J. D. Protasiewicz, *J. Am. Chem. Soc.*, 2001, **123**, 6925–6926; (*b*) T. Kyoko, F. Yuuichi, S. Shigeru and Y. Masaaki, *Chem. Lett.*, 1997, **26**, 855–856; (*c*) T. Sasamori, N. Takeda and N. Tokitoh, *J. Phys. Org. Chem.*, 2003, **16**, 450–462; (*d*) N. Nagahora, T. Sasamori, N. Takeda and N. Tokitoh, *Chem.–Eur. J.*, 2004, **10**, 6146–6151; (*e*) K. Tsuji, S. Sasaki and M. Yoshifuji, *Heteroat. Chem.*, 1998, **9**, 607–613; (*f*) E. Urnéžius and J. D. Protasiewicz, *Main Group Chem.*, 1996, **1**, 369–372.

18 R. Pietschnig and E. Niecke, *Organometallics*, 1996, **15**, 891–893.

19 (*a*) V. B. Gudimetla, A. L. Rheingold, J. L. Payton, H.-L. Peng, M. C. Simpson and J. D. Protasiewicz, *Inorg. Chem.*, 2006, **45**, 4895–4901; (*b*) T. H. Lowry and K. S. Richardson, *Mechanism and Theory in Organic Chemistry*, Harper and Row, New York, 1981.

20 (*a*) J. L. Magee, W. Shand and H. Eyring, *J. Am. Chem. Soc.*, 1941, **63**, 677–688; (*b*) E. R. Talaty and J. C. Fargo, *Chem. Commun.*, 1967, 65–66; (*c*) M. Calvin and H. W. Alter, *J. Chem. Phys.*, 1951, **19**, 768–770; (*d*) J.-Å. Andersson, R. Petterson and L. Tegnér, *J. Photochem.*, 1982, **20**, 17–32.

21 (*a*) G. B. Kistiakowsky and W. R. Smith, *J. Am. Chem. Soc.*, 1934, **56**, 638–642; (*b*) C. Bastianelli, V. Caia, G. Cum, R. Gallo and V. Mancini, *J. Chem. Soc., Perkin Trans. 2*, 1991, 679–683.

22 G. S. Hartley, *J. Chem. Soc.*, 1938, 633–642.

23 M. J. Frisch, *et al.*, *Gaussian 16, Revision C.01*, 2016.

24 (*a*) H.-L. Peng, J. L. Payton, J. D. Protasiewicz and M. C. Simpson, *Dalton Trans.*, 2012, **41**, 13204–13209; (*b*) T. Copeland, M. P. Shea, M. C. Milliken, R. C. Smith, J. D. Protasiewicz and M. C. Simpson, *Anal. Chim. Acta*, 2003, **496**, 155–163.

25 (*a*) M. Yoshifuji, T. Hashida, N. Inamoto, K. Hirotsu, T. Horiuchi, T. Higuchi, K. Ito and S. Nagase, *Angew. Chem., Int. Ed.*, 1985, **24**, 211–212; (*b*) S. Sinha Ray, *Chem. Phys.*, 2020, **529**, 110555; (*c*) T. Lu, A. C. Simmonett, F. A. Evangelista, Y. Yamaguchi and H. F. Schaefer III, *J. Phys. Chem. A*, 2009, **113**, 13227–13236.

26 (*a*) D. V. Partyka, M. P. Washington, T. G. Gray, J. B. Updegraff Iii, J. F. Turner II and J. D. Protasiewicz, *J. Am. Chem. Soc.*, 2009, **131**, 10041–10048; (*b*) A. Tsurusaki, R. Ura and K. Kamikawa, *Organometallics*, 2020, **39**, 87–92.

27 (*a*) J. Chatt, P. B. Hitchcock, A. Pidcock, C. P. Warrens and K. R. Dixon, *J. Chem. Soc., Dalton Trans.*, 1984, 2237–2244; (*b*) R. A. Jones, M. H. Seeberger and B. R. Whittlesey, *J. Am. Chem. Soc.*, 1985, **107**, 6424–6426; (*c*) H. Krautscheid, E. Matern, G. Fritz and J. Pikies, *Z. Anorg. Allg. Chem.*, 2000, **626**, 253–257; (*d*) S. Sabater, D. Schmidt, H. Schmidt, M. W. Kuntze-Fechner, T. Zell, C. J. Isaac, N. A. Rajabi, H. Grieve, W. J. M. Blackaby, J. P. Lowe, S. A. Macgregor, M. F. Mahon, U. Radius and M. K. Whittlesey, *Chem.–Eur. J.*, 2021, **27**, 13221–13234; (*e*) S. Gómez-Ruiz, S. Zahn, B. Kirchner, W. Böhlmann and E. Hey-Hawkins, *Chem.–Eur. J.*, 2008, **14**, 8980–8985; (*f*) I. G. Phillips, R. G. Ball and R. G. Cavell, *Inorg. Chem.*, 1992, **31**, 1633–1641; (*g*) M. K. Sharma, D. Rottschäfer, B. Neumann, H.-G. Stammler, S. Danés, D. M. Andrada, M. van Gastel, A. Hinz and R. S. Ghadwal, *Chem.–Eur. J.*, 2021, **27**, 5803–5809; (*h*) S. Gómez-Ruiz and E. Hey-Hawkins, *Dalton Trans.*, 2007, 5678–5683; (*i*) N. Nagahora, T. Sasamori and N. Tokitoh, *Organometallics*, 2008, **27**, 4265–4268; (*j*) S. Kurz and E. Hey-Hawkins, *J. Organomet. Chem.*, 1993, **462**, 203–207; (*k*) D. Fenske and K. Merzweiler, *Angew. Chem., Int. Ed.*, 1984, **23**, 635–637.

28 P. Jutzi and S. Opiela, *Z. Anorg. Allg. Chem.*, 1992, **610**, 75–82.

29 G. S. Hartley, *Nature*, 1937, **140**, 281.

30 L. Y. M. Eymann, P. Varava, A. M. Shved, B. F. E. Curchod, Y. Liu, O. M. Planes, A. Sienkiewicz, R. Scopelliti, F. Fadaei Tirani and K. Severin, *J. Am. Chem. Soc.*, 2019, **141**, 17112–17116.